

Environmental impact of geometric earthwork construction in pre-Columbian Amazonia

Article

Accepted Version

Carson, J. F., Whitney, B. S., Mayle, F. E. ORCID: <https://orcid.org/0000-0001-9208-0519>, Iriarte, J., Prümers, H., Soto, J. D. and Watling, J. (2014) Environmental impact of geometric earthwork construction in pre-Columbian Amazonia. *Proceedings of the National Academy of Sciences of the United States of America*, 111 (29). pp. 10497-10502. ISSN 0027-8424 doi: <https://doi.org/10.1073/pnas.1321770111> Available at <https://centaur.reading.ac.uk/37135/>

It is advisable to refer to the publisher's version if you intend to cite from the work. See [Guidance on citing](#).

Published version at: <http://www.pnas.org/content/early/2014/07/03/1321770111>

To link to this article DOI: <http://dx.doi.org/10.1073/pnas.1321770111>

Publisher: National Academy of Sciences

All outputs in CentAUR are protected by Intellectual Property Rights law, including copyright law. Copyright and IPR is retained by the creators or other copyright holders. Terms and conditions for use of this material are defined in the [End User Agreement](#).

www.reading.ac.uk/centaur

CentAUR

Central Archive at the University of Reading

Reading's research outputs online

Environmental impact of geometric earthwork construction in pre-Columbian Amazonia

John Francis Carson^{a,b,1}, Bronwen S. Whitney^b, Francis E. Mayle^a, José Iriarte^c, Heiko Prümers^d, J. Daniel Soto^e, and Jennifer Watling^c

^aDepartment of Geography and Environmental Science, University of Reading, Whiteknights, Reading RG6 6AB, United Kingdom; ^bSchool of GeoSciences, University of Edinburgh, Edinburgh EH8 9XP, United Kingdom; ^cDepartment of Archaeology, University of Exeter, Exeter EX4 4QE, United Kingdom; ^dKommission für Archäologie Aussereuropäischer Kulturen, Deutsches Archäologisches Institut, 53173 Bonn, Germany; and ^eHerbario del Oriente Boliviano, Museo de Historia Natural 'Noel Kempff Mercado,' Universidad Autónoma Gabriel René Moreno, Casilla 2489, Santa Cruz, Bolivia

Abstract

There is considerable controversy over whether pre-Columbian (pre-A.D. 1492) Amazonia was largely “pristine” and sparsely populated by slash-and-burn agriculturists, or instead a densely populated, domesticated landscape, heavily altered by extensive deforestation and anthropogenic burning. The discovery of hundreds of large geometric earthworks beneath intact rainforest across southern Amazonia challenges its status as a pristine landscape, and has been assumed to indicate extensive pre-Columbian deforestation by large populations. We tested these assumptions using coupled local- and regional-scale paleoecological records to reconstruct land use on an earthwork site in northeast Bolivia within the context of regional, climate-driven biome changes. This approach revealed evidence for an alternative scenario of Amazonian land use, which did not necessitate labor-intensive rainforest clearance for earthwork construction. Instead, we show that the inhabitants exploited a naturally open savanna landscape that they maintained around their settlement despite the climatically driven rainforest expansion that began ~2,000 y ago across the region. Earthwork construction and agriculture on terra firme landscapes currently occupied by the seasonal rainforests of southern Amazonia may therefore not have necessitated large-scale deforestation using stone tools. This finding implies far less labor—and potentially lower population density—than previously supposed. Our findings demonstrate that current debates over the magnitude and nature of pre-Columbian Amazonian land use, and its impact on global biogeochemical cycling, are potentially flawed because they do not consider this land use in the context of climate-driven forest–savanna biome shifts through the mid-to-late Holocene.

Introduction

Evidence for the existence of large and socially complex societies in Amazonia before the arrival of Europeans (pre-A.D. 1492) is emerging from a growing number of archaeological sites across the Amazon Basin (1–9). The scale of these societies' environmental impact and its potential legacy in modern Amazonian forest ecosystems are hotly debated. Whereas some argue for a relatively limited and localized human influence (10–13), others have described pre-Columbian Amazonia as a “cultural parkland,” which was widely impacted by human disturbance (14–16). It has been proposed that deforestation and biomass burning before the collapse of native Amazonian populations following European contact in A.D. 1492 occurred on a scale large enough to contribute to an early anthropogenic influence on the global carbon cycle (17), and was a significant forcing of Holocene climate perturbations (18). It has also been suggested that this pervasive historical human influence on Amazonian forest ecosystems should change our views on their resilience to human impacts and influence our approach to their conservation (19). However, in many regions, a lack of appropriately scaled palaeoecological data means that we have no palaeoenvironmental context in which to place these societies and assess their environmental impacts.

Paleoecological studies (20–23) conducted in aseasonal western and central Amazonia suggest stability of the rainforest biome throughout the Holocene and appear to show little evidence for significant deforestation or biomass burning by their pre-Columbian inhabitants. However, the presence of regionally extensive pre-Columbian geometric earthworks underlying the seasonal southern Amazonian rainforests (SSAR) (Fig. 1A) (2,4, 15, 24, 25) is suggestive of large-scale historical deforestation by substantial populations. These earthworks, uncovered by modern deforestation, are thought to represent only a fraction of the total, which lie undiscovered beneath the intact SSAR (3), a subregion of ~1,000,000 km² (SI Text, Site Descriptions), which constitutes one-fifth of the Amazon basin. This practice of geometric earthwork building appears to have developed and diverged across southern Amazonia over a long time period from prehistory to European contact (2) (SI Text, Geometric Earthworks).

Here we investigated the environmental impact of geometric earthwork building by using paleoecological techniques to reconstruct vegetation change and human land use on both a local and a regional scale around a pre-Columbian earthwork site in northeast Bolivia.

Study Area

Our study was conducted in Iténez province in northeast Bolivia at the geologically defined boundary between the terra firme (non-flooded) humid evergreen rainforest on the uplands of the pre-Cambrian Shield (PCS) and the seasonally flooded savannahs of the adjacent Beni sedimentary basin (31). Although the forest– savanna boundary of our study area is locally controlled by geological, edaphic, and hydrological conditions, it is situated well within the SSAR, the southern ecotone of which is controlled by precipitation at a broad regional scale (Fig. 1A). Archaeologically, the Iténez region is characterized by extensive networks of artificial earthworks covering an estimated area of 12,000 km² (24). On the terra firme land of the PCS, these include dense clusters of ring ditches, ranging from circular forms, up to several hundred meters in diameter, to kilometer-long curvilinear ditches up to 3-m deep and 4-m wide. The function of these ring ditches is unknown. One possibility is that they acted as defensive features around settlements and were perhaps enhanced by the construction of palisade walls built from tree trunks (24). However, no archaeological evidence of post holes or wood remains has yet been found to confirm this hypothesis (32). Other suggested functions for geometric earthworks include: drainage (5), ceremonial/religious (3), or formal organization of space according to social hierarchy (1, 15).

To gain a temporal understanding of the nature and scale of human impact on vegetation in the ring-ditch region of northeast Bolivia, we analyzed fossil pollen and macroscopic charcoal from radiocarbon-dated lake sediment cores to reconstruct palaeovegetation and fire history over the past ~6,000 y (Methods). The pollen source area represented by fossil pollen in lake sediments is determined by lake surface area (33). We therefore selected a pair of lakes of contrasting size to capture vegetation on two distinct spatial scales (Fig. 1B). The smaller of the two lakes, Laguna Granja (LG), reflects local-scale vegetation at an adjacent ring-ditch site (Fig. 1C) and is nested within the regional-scale pollen catchment of the much larger lake, Laguna Orícore (LO), which reveals broader, biome-scale vegetation changes on the PCS (SI Text, Pollen catchment area).

During the rainy season, both lakes receive flood waters (and hence pollen input) from the surrounding seasonally flooded savannahs of the Beni basin, as well as from the adjacent San Martín river, which drains rainforest, dry forest, and savannah regions south of Iténez. However, despite this floodwater input, we found that the surface-sediment pollen assemblages of both lakes were dominated by taxa indicative of the terra firme humid evergreen rainforest that covers the PCS. Our interpretation is based upon extensive modern pollen rain studies conducted in the Bolivian Amazon, which enabled us to distinguish between the characteristic pollen signatures of savanna, seasonally dry tropical forest, and humid evergreen rainforest (34–37). Most of the pollen entering the two lakes

must therefore originate via wind dispersal from the vegetation of the PCS, with only a background input from the Beni basin and riverine flood waters. Analysis of the fossil pollen and macroscopic charcoal from the deeper lake sediments confirms that the paleoecological records from our study lakes are representative of changes in the ring-ditch region in northern Iténez and not the region to the south drained by the San Martín river (*SI Text, Pollen and charcoal source*).

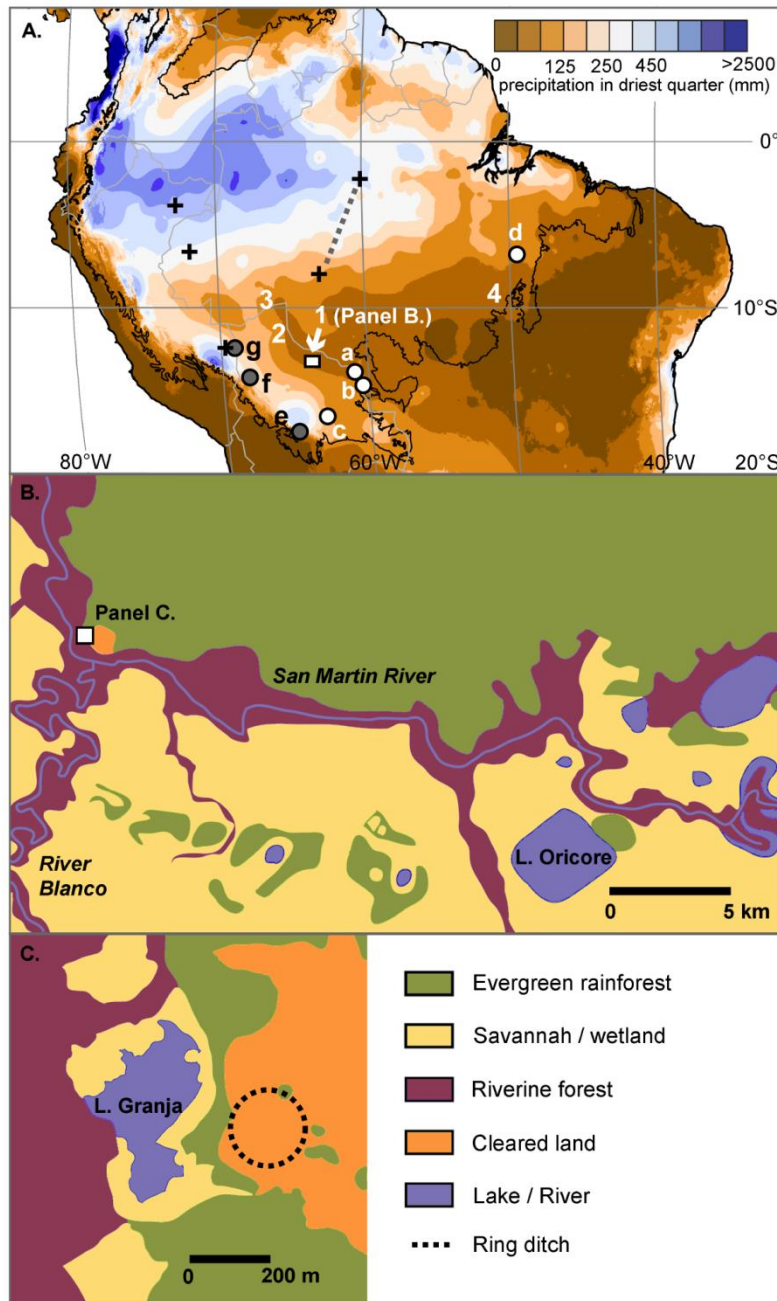


Fig. 1. Map of site locations. (A) Present-day precipitation across Amazon basin during the three driest months of the year (26); solid black line delimits modern extent of Amazonian forest; approximate extent of SSAR/geometric earthwork region is within the <125-mm isohyet. Over 400 geometric earthworks have been discovered in eastern Acre, Brazil (location no. 3 in A), and many more across Iténez (location no. 1 in A, detail in B) and Riberalta (location no. 2 in A), northeast

Bolivia, and the Upper Xingu (location no. 4 in A), Brazil. Previously published lake-sediment pollen records showing evidence for late Holocene biome shifts are represented by white circles: (a) Bella Vista, (b) Chaplin (27), (c) Yaguarú (28), (d) Carajas (29). Previously published lake-sediment pollen records in central and western Amazonia, which show stability of the forest biome and limited or no human impact over mid-to-late Holocene, are represented by gray circles: (e) Siberia (30), (f) Chalalán and Santa Rosa (22), (g) Gentry, Parker, Vargas, Werth (23). Black crosses represent soil-pit sampling locations/transects discussed in the main text, which show little evidence of pre-Columbian forest disturbance (20, 21). (B) Study area showing locations of LO and LG (detail in C), main rivers, and biome distribution. (C) Laguna Granja and Granja del Padre ring ditch.

Results and interpretation

L. Orícore. In zone LO-1 (5700–2000 calibrated years before present, or cal yr B.P.) (Fig. 2), LO shows low arboreal pollen levels ($\leq 30\%$) and high Poaceae (grass) abundance (up to 50%), which— together with peak abundance of drought-tolerant taxa, such as *Anadenanthera*, and maximum charcoal concentrations—indicate a drier and regionally more open environment compared with the present (34–37). At the zone LO-1/LO-2 boundary (~ 2000 cal yr B.P.), total arboreal pollen percentages begin to increase, with especially marked increases in abundance of evergreen taxa, such as *Brosimum* and *Alchornea*, whereas Poaceae, *Anadenanthera*, and charcoal levels decline, signalling an expansion of closed-canopy humid evergreen rainforest (34–36). By ~ 1700 cal yr B.P., total arboreal pollen percentages had reached modern values, indicating that the regional terra firme PCS landscape had reached a level of forest cover comparable to the modern closed-canopy rainforest. This record of a savanna landscape changing to evergreen rainforest ~ 2000 cal yr B.P. is consistent with paleoecological studies from other parts of southern Amazonia, which were dominated by savanna and seasonally dry tropical forest until ~ 3000 – 2000 B.P., when humid evergreen rainforest began to expand southward (27–29). These records of expanding evergreen rainforest coincide with increasing lake levels at Lake Titicaca (38, 39) (an Andean site that receives most of its precipitation from lowland Amazonia), suggesting that rainforest expansion occurred as a result of increasing precipitation across southern Amazonia. The latter reflects a strengthening of the South American summer monsoon, driven by increased insolation linked to precessional orbital forcing (27). Further independent, multiproxy evidence of mid-to-late Holocene climate change in the study area is presented in *SI Text, Mid-Late Holocene Climate Change*.

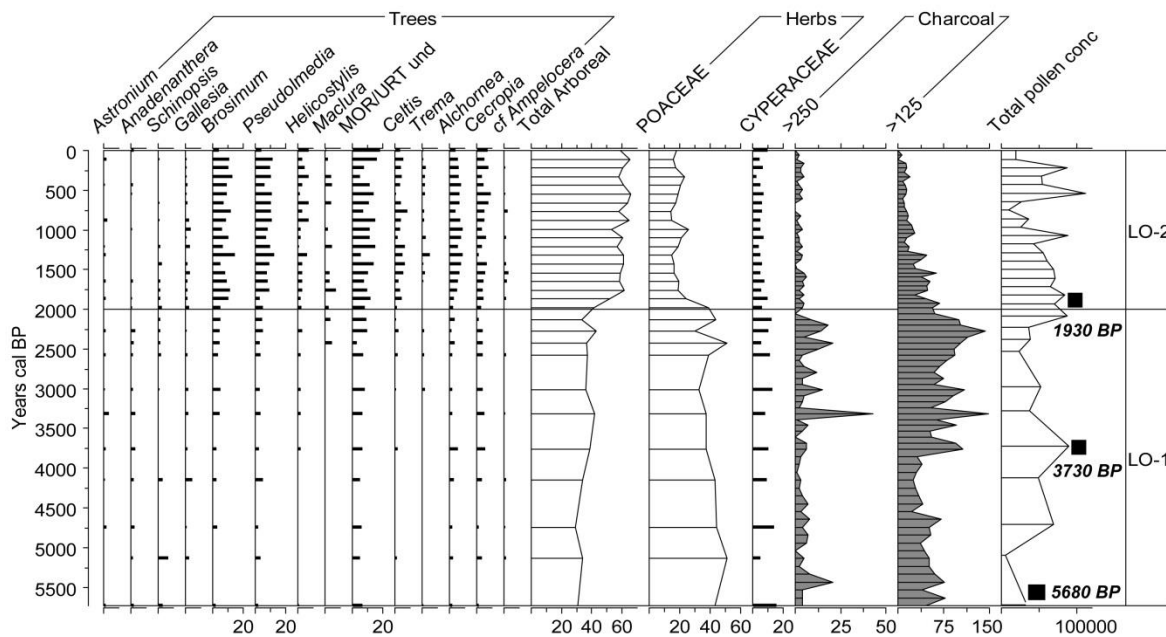


Fig. 2. L. Orícore pollen and charcoal records. Pollen data presented as percent abundance (of the total terrestrial pollen sum) and total concentrations per cm^3 . Charcoal presented as particles/ cm^3 . “Total Arboreal” is the sum of all tree taxa ($> 2\%$ abundance) are shown. Plotted against calibrated radiocarbon years BP and individual radiocarbon dates shown on right (See table S1 and figure S1).

L. Granja. LG provides a record of local-scale human impact at a ring ditch site on the PCS, on the outskirts of the modern day town of Bella Vista (*SI Text, Site Descriptions*). Ground mapping and airborne light detection and ranging (LiDAR) surveys conducted by H.P. over an area of 200 km^2 around LG have documented numerous earthworks enclosing areas up to 200 ha. Two ring ditches, one located 100 m east of the lake and the second located 1 km away, have been radiocarbon dated to between ~ 800 and 500 cal yr B.P. (40). The ring ditch nearest to the lake (Fig. 3) is 150 m in diameter and 2 m deep, and is connected to the second ring ditch by a linear ditch that bisects an area of 150 ha. Excavations of this nearest ring ditch uncovered 15 separate burials and associated ceramics.



Fig. 3. Aerial photo of ring ditch next to LG (taken 2008 by H.P.). Open ground around the ditch reflects modern, small-scale clearance for cattle pasture.

In zone LG-1 the high ratio of Poaceae to arboreal pollen (Fig. 4) (6100–2500 cal yr B.P.) shows that, before occupation, the environment around LG was an open savanna, in contrast to the dense evergreen rainforest that exists there today (notwithstanding scattered clearings made for cattle pasture and slash-and-burn agriculture), an interpretation reinforced by modern pollen-vegetation studies (34–37). The LG-1/LG-2 zone boundary marks the onset of agriculture and anthropogenic burning at LG at 2500 cal yr B.P., as indicated by a sharp charcoal increase and the presence of maize pollen (*Zea mays* L.). Although the charcoal record shows variations, with two distinct periods of more intensive anthropogenic burning at ~2500–1600 cal yr B.P. and ~700–500 cal yr B.P., the almost continual presence of maize pollen shows that the site was occupied throughout zones LG-2 and LG-3. The second charcoal peak (700–500 cal yr B.P.) coincides with peak Poaceae pollen percentages and ring ditch construction/occupation (~800–500 cal yr B.P.) (40), which indicates, either a more intense period of burning associated with the ring ditch construction, or burning closer to the lake itself (*SI Text, L. Granja charcoal*). The decrease in arboreal types at this horizon is driven mostly by the disappearance of taxa such as *Alchornea*, *Celtis*, and *Cecropia*, indicating clearance of the gallery forest immediately around the lake (34–36). Open savanna/ grassland vegetation persists throughout zone LG-2 and expansion of dense-canopy rainforest into the terra firme around LG does not occur until ~500 cal yr B.P. (zone LG-2/3 boundary) following a decline in human activity at the site, possibly linked to the introduction of Old World diseases associated with the arrival of Europeans in the Americas in A.D. 1492 (41).

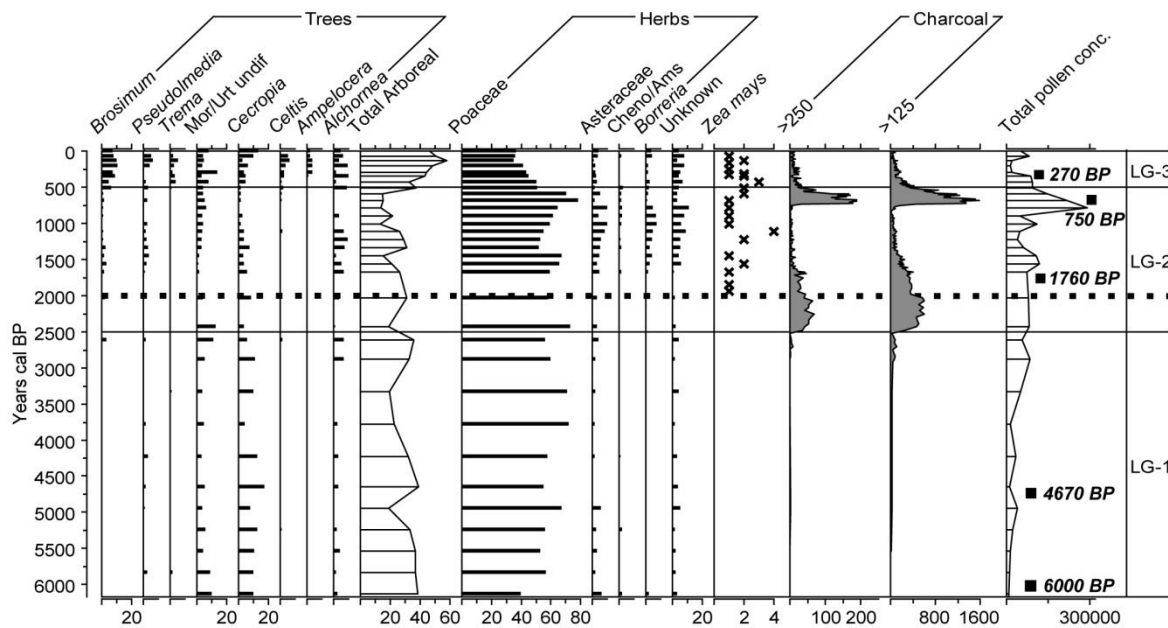


Fig. 4. L. Granja pollen and charcoal records. Pollen data presented as percent abundance (of the total terrestrial pollen sum) and total pollen concentrations. Charcoal presented as particles/cm³. *Zea mays* plotted as no. of grains per ~0.4 cm³. “Total Arboreal” is the sum of all tree taxa. Dominant tree pollen types (>2% abundance) are shown. Dashed line indicates timing of regional forest expansion shown in LO. Plotted against calibrated years BP, with individual radiocarbon dates shown on the right (see table S1 and figure S2).

The timing of this local forest expansion at LG (~500 cal yr B.P.) contrasts with the much earlier regional-scale pattern of forest expansion seen at LO (~2000 cal yr B.P.). The most parsimonious explanation for the persistence of this open landscape at LG is that early settlers maintained open ground on a local scale by suppressing forest expansion around the settlement. The maintenance of this opening is not seen in the LO record because the much larger pollen catchment area of LO means that it is insensitive to detecting openings on the scale of the ring-ditch site (33). The LG pollen record therefore demonstrates that construction of the earthworks and agricultural activity around LG occurred in an open environment, maintained since the first occupation of the site. Rather than having to rely upon stone axes and burning to clear dense-canopy rainforest, a feat that would have been hugely labor intensive and highly impractical before the introduction of steel tools (42), our data show that the inhabitants took advantage of an existing open savanna landscape. Although the movement of earth to construct the ring ditches would have required a considerable labor force, the maintenance of an open landscape locally around LG, by the suppression of tree growth associated with the climate-driven rainforest expansion, would have required far less human effort (and potentially a lower population density) than that needed for the removal of dense-canopy rainforest.

Implications

It is intriguing that most geometric earthworks found beneath terra firme tropical forest have been concentrated in seasonal southern Amazonia [i.e., northeast Bolivia (4, 24), eastern Acre state (3, 25), and the upper Xingu region of Brazil (15)], rather than wetter, less seasonal parts of the basin (Fig. 1A). Late Holocene climate-driven rainforest expansion has been documented in other parts of southern Amazonia (27–29), coinciding with rising lake levels in the tropical Andes (38, 39), which demonstrates that the forest expansion at LO reflects a broad-scale vegetation response to increasing precipitation across the southern Amazon. However, the geographic scale of this biome shift in the context of large geometric earthwork construction has hitherto not been considered. Our discovery raises the strong possibility that other geometric earthworks across southern Amazonia were also built in a savanna/open woodland that subsequently became covered by closed-canopy forest. Although dating of two of the numerous ring ditches at the Bella Vista site has shown them to be relatively late features (built and occupied between ~800 and 500 B.P.), geometric earthworks in Pando (northeast Bolivia) and eastern Acre (northwest Brazil) have been dated to as early as 2000 B.P. (4, 43). The recent discovery of ancient shell middens in the central Beni basin have demonstrated a human presence in the Bolivian Amazon since the early Holocene (~10,000 y B.P.) (44).

Gaining a sound understanding of the historical role of humans in shaping Amazonian landscapes, and the extent to which Amazonian forests were resilient to historical disturbance, is critical to informing policy makers on sustainable Amazonian futures (8, 12, 16, 19, 45). However, the debate so far has considered only the extent of past human impact and land use in what is assumed to have been a forested landscape, based upon the modern distribution of forest. Our study demonstrates that current debates over the magnitude and nature of pre-Columbian Amazonian land use are potentially flawed because they do not consider this land use in the context of climate-driven ecosystem dynamics through the mid-to-late Holocene (27, 29). Our findings show that, to determine the scale of environmental impact associated with pre-Columbian land use, the type of vegetation cover (e.g., closed-canopy forest versus open woodland or savanna) antecedent to settlement must first be known. This is a vital prerequisite to drawing inferences regarding population size and subsistence strategies.

Our findings have implications too for the debate over the scale of pre-Columbian impacts upon biogeochemical cycling. It has been speculated that post-Columbian secondary forest regrowth and the reduction in biomass burning across the Neotropics following indigenous population collapse caused sufficient carbon sequestration to reduce atmospheric CO₂ concentrations (17, 46) and amplify Little Ice Age cooling (17). It has also been suggested that observed biomass gains among old-growth lowland Neotropical forests over recent decades may be because of continued recovery from pre-Columbian anthropogenic disturbance (47). Our data support an alternative scenario, whereby pre-Columbian terra firme agriculture and construction of vast and numerous earthworks did not

necessitate large-scale deforestation. On a regional scale, forest expansion in the SSAR occurred largely in response to increasing precipitation over the past 2,000 y, rather than solely as part of a vast post-disturbance forest recovery over the last 500 y following indigenous population collapse. However, superimposed upon this broad-scale, climate-driven, biome shift, humans did have significant environmental impact on a more local scale by suppressing climate driven forest expansion around occupation sites. In the case of LG, its occupants held back rainforest expansion around the site for ~1,500 y until a probable population collapse ~500 cal yr B.P., possibly associated with European contact, allowing afforestation to occur. This new scenario of pre-Columbian land use fits neither of the opposing views of the current debate, which pits a model of short-lived, small-scale forest disturbance against a model of large-scale deforestation. Instead, we posit a more complex interaction between climatically driven ecosystem changes and long-term human land-use strategies. This new model does not preclude the possibility that Amazonian geometric earthwork building cultures may also have impacted their environment in more subtle ways, for example, by altering the floristic composition of forest through management of economically valuable taxa and modifying soil conditions. Further palaeoecological work and close integration with archaeological data are required to better understand the nature of pre-Columbian land-use strategies in southern Amazonia and their possible involvement in the development of the rainforest ecosystem of this region following forest expansion in recent millennia.

Methods

The LG core was subsampled for pollen analysis at 5-cm intervals between 0- and 110-cm depth (0 to ~3300 cal yr B.P.) and at 10-cm intervals between 110- and 150-cm depth (3300 to ~6100 cal yr B.P.). The LO core was subsampled at 1-cm intervals between 0- and 22-cm depth (0 to ~2550 cal yr B.P.) to capture the savanna–forest transition at high resolution, and at 2- to 3-cm intervals between 22- and 40-cm depth (~2550 to ~6700 cal yr B.P.). Samples were prepared using standard laboratory protocol (48) and separated into a fine (<53 μm) and a coarse fraction (>53 μm) for optimal recovery of large cultigen pollen (49). Calculation of pollen concentration confirmed that observed changes in pollen percentage abundance in the paleo record were not the result of changes within a closed sum (SI Text, Pollen concentration values). The pollen in the fine fractions was counted to the standard 300 terrestrial grains. The coarse fractions were scanned up to a standardized equivalent count of 2,000 Lycopodium grains, representing ~0.4 cm³ of sediment scanned. Fossil pollen was identified with reference to the collection of over 1,000 tropical pollen specimens housed at the University of Edinburgh and University of Reading. Maize pollen grains were distinguished from those of other wild grasses according to the morphological criteria described in Holst et al. (50). Where possible, members of the Moraceae family were identified to genus using pollen reference material and morphological descriptions from Burn and Mayle (51). LG was subsampled for

macroscopic charcoal analysis at every 0.5-cm interval from 0- to 110-cm depth, and in the remainder of the core where charcoal abundance was consistently low, sampling resolution was lowered to 5-cm intervals. LO was subsampled at 0.5-cm intervals from 0- to 40-cm depth. *See SI Methods and Figs. S1–S5* for more detailed descriptions.

ACKNOWLEDGMENTS.

We thank Douglas Bruckner of the ‘Programa de Conservación de la Paraba Barba Azul’; the rangers from the ‘Reserva Iténez’ WWF station, for logistical support in the field; and José Manuel Barrios Fernández for allowing us access to core the Granja del Padre site. This research was supported by Leverhulme Trust research Grant F/00158/Ch (to F.E.M. and J.I.); Natural Environment Research Council (NERC) Doctoral Training Scheme Grant NE/152830X/1(to J.F.C.); and funds from the University of Edinburgh’s Principal’s Career Development scholarship (J.F.C.). An NERC radiocarbon facility date (1623.0312) was granted to F.E.M. Fieldwork support was provided by the Noel Kempff Mercado Natural History Museum.

References

1. Heckenberger MJ, et al. (2008) Pre-Columbian urbanism, anthropogenic landscapes, and the future of the Amazon. *Science* 321(5893):1214–1217.
2. Schaan DP (2012) *Sacred Geographies of Ancient Amazonia: Historical Ecology of Social Complexity* (Left Coast Press, Walnut Creek, CA).
3. Parssinen M, Schaan D, Ranzi A (2009) Pre-Columbian geometric earthworks in the upper Purús: A complex society in western Amazonia. *Antiquity* 83(322):1084–1095.
4. Saunaluoma S (2010) Pre-Columbian earthworks in the Riberalta region of the Bolivian Amazon. *Amazonica* 2(1):104–138.
5. Walker JH (2008) Pre-Columbian ring ditches along the Yacunta and Rapulo rivers, Beni, Bolivia: A preliminary review. *J Field Archaeol* 33(4):413–427.
6. Denevan WM (1966) *The Aboriginal Cultural Geography of the Llanos de Mojos of Bolivia* (Univ of California Press, Berkley).
7. Roosevelt A (1991) *Moundbuilders of the Amazon: Geophysical Archaeology on Marajo Island, Brazil* (San Diego Academic Press, San Diego).
8. Iriarte J, et al. (2012) Fire-free land use in pre-1492 Amazonian savannas. *Proc Natl Acad Sci USA* 109(17):6473–6478.
9. Heckenberger MJ, Neves EG (2009) Amazonian archaeology. *Annu Rev Anthropol* 38: 251–266.
10. Meggers B (1992) in *Disease and Demography in the Americas*, eds Verano JW, Uberlaker DH (Smithsonian Institution, Washington, DC), pp 197–205.
11. Bush MB, Silman M (2007) Amazonian exploitation revisited: Ecological asymmetry and the policy pendulum. *Front Ecol Environ* 5(9):457–465.
12. Barlow J, Gardner TA, Lees AC, Parry L, Peres CA (2012) How pristine are tropical forests? An ecological perspective on the pre-Columbian human footprint in Amazonia and implications for contemporary conservation. *Biol Conserv* 151(1):45–49.
13. Peres CA, et al. (2010) Biodiversity conservation in human-modified Amazonian forest landscapes. *Biol Conserv* 143(10):2314–2327.
14. Erickson C, Balée W (2006) in *Time and Complexity in Historical Ecology: Studies in the Neotropical Lowlands*, eds Balee W, Erickson CL (Columbia Univ Press, New York), pp 187–233.
15. Heckenberger MJ, et al. (2003) Amazonia 1492: Pristine forest or cultural parkland? *Science* 301(5640):1710–1714.
16. Clement CR, Junqueira AB (2010) Between a pristine myth and an impoverished future. *Biotropica* 42(5):534–536.
17. Nevle RJ, Bird DK, Ruddiman WF, Dull RA (2011) Neotropical human-landscape interactions, fire, and atmospheric CO₂ during European conquest. *Holocene* 21(5):853–864.

18. Dull RA, et al. (2010) The Columbian encounter and the Little Ice Age: Abrupt land use change, fire, and greenhouse forcing. *Ann Assoc Am Geogr* 100(4):755–771.
19. Heckenberger MJ, Russell JC, Toney JR, Schmidt MJ (2007) The legacy of cultural landscapes in the Brazilian Amazon: Implications for biodiversity. *Philos Trans R Soc Lond B Biol Sci* 362(1478):197–208.
20. McMichael CH, et al. (2012) Sparse pre-Columbian human habitation in western Amazonia. *Science* 336(6087):1429–1431.
21. McMichael CH, et al. (2011) Spatial and temporal scales of pre-Columbian disturbance associated with western Amazonian lakes. *Holocene* 22(2):131–141.
22. Urrego DH, et al. (2013) Holocene fires, forest stability and human occupation in southwestern Amazonia. *J Biogeogr* 40(3):521–533.
23. Bush MB, et al. (2007) Holocene fire and occupation in Amazonia: Records from two lake districts. *Philos Trans R Soc Lond B Biol Sci* 362(1478):209–218.
24. Erickson C (2010) The transformation of environment into landscape: The historical ecology of monumental earthwork construction in the Bolivian Amazon. *Diversity* 2(4):618–652.
25. Mann CC (2008) Archaeology. Ancient earthmovers of the Amazon. *Science* 321(5893):1148–1152.
26. Hijmans RJ, Cameron SE, Parra JL, Jones PG, Jarvis A (2005) Very high resolution interpolated climate surfaces for global land areas. *Int J Climatol* 25(15):1965–1978.
27. Mayle FE, Burbridge R, Killeen TJ (2000) Millennial-scale dynamics of southern Amazonian rain forests. *Science* 290(5500):2291–2294.
28. Taylor ZP, Horn SP, Mora CI, Orvis KH, Cooper LW (2010) A multi-proxy palaeoecological record of late-Holocene forest expansion in lowland Bolivia. *Palaeogeogr Palaeoclimatol Palaeoecol* 293(1-2):98–107.
29. Absy ML, et al. (1991) Mise en évidence de quatre phases d'ouverture de la forêt dense dans le sud-est de l'Amazonie au cours des 60,000 dernières années. Première comparaison avec d'autres régions tropicales [Highlighting four phases of opening of the dense forest in south-east Amazonia over the last 60,000 years. First comparison with other tropical regions.]. *Compt Rend Acad des Sci Paris Ser II* 312:673–678.
30. Mourguiart P, Ledru M-P (2003) Last Glacial Maximum in an Andean cloud forest environment (Eastern Cordillera, Bolivia). *Geology* 31(3):195–198.
31. Navarro G, Maldonado M (2005) *Geografía Ecología de Bolivia: Vegetación y Ambientes Acuáticos* [Ecological Geography of Bolivia: Vegetation and Aquatic Environments] (Centro de ecología difusión de simion I, Patino, Santa Cruz, Bolivia). Spanish.
32. Prümers H (2013) Die arbeiten des Bolivianisch-Deutschen Projektes in Mojos in den jahren 2011 / 2012 [The work of the Bolivian-German Project in the Mojos in the years 2011–2012]. *Zeitschrift für Archaeol Aussereuropaischer* 5:315–324.
33. Sugita S (1994) Pollen representation of vegetation in Quaternary sediments: Theory and method in patchy vegetation. *J Ecol* 82(4):881–897.

34. Burn M, Mayle FE, Killeen T (2010) Pollen-based differentiation of Amazonian rainforest communities and implications for lowland palaeoecology in tropical South America. *Palaeogeogr Palaeoclimatol Palaeoecol* 295(1-2):1–18.
35. Gosling W, Mayle FE, Tate N, Killeen T (2005) Modern pollen-rain characteristics of tall terra firme moist evergreen forest, southern Amazonia. *Quat Res* 64(3):284–297.
36. Gosling W, Mayle FE, Tate N, Killeen T (2009) Differentiation between Neotropical rainforest, dry forest, and savannah ecosystems by their modern pollen spectra and implications for the fossil pollen record. *Rev Palaeobot Palynol* 153(1-2):70–85.
37. Jones H, Mayle FE, Pennington RT, Killeen T (2011) Characterisation of Bolivian savanna ecosystems by their modern pollen rain and implications for fossil pollen records. *Rev Palaeobot Palynol* 164(3-4):223–237.
38. Baker PA, et al. (2001) The history of South American tropical precipitation for the past 25,000 years. *Science* 291(5504):640–643.
39. Cross S, Baker P, Seltzer GO, Fritz SC, Dunbar RB (2000) A new estimate of the Holocene lowstand level of Lake Titicaca, central Andes, and implications for tropical palaeohydrology. *Holocene* 10(1):21–32.
40. Dickau R, et al. (2012) Diversity of cultivars and other plant resources used at habitation sites in the Llanos de Mojos, Beni, Bolivia: Evidence from macrobotanical remains, starch grains, and phytoliths. *J Archaeol Sci* 39(2):357–370.
41. Denevan WM (1992) The Pristine Myth: The landscape of the Americas in 1492. *Ann Assoc Am Geogr* 82(3):369–385.
42. Denevan WM (2001) *Cultivated Landscapes of Native Amazonia and the Andes* (Oxford Univ Press, Oxford).
43. Schaan D, et al. (2012) New radiometric dates for pre-Columbian (2000–700 B.P.) earthworks in western Amazonia, Brazil. *J Field Archaeol* 37(2):132–142.
44. Lombardo U, et al. (2013) Early and middle Holocene hunter-gatherer occupations in western Amazonia: The hidden shell middens. *PLoS ONE* 8(8):e72746.
45. Renard D, et al. (2012) Ecological engineers ahead of their time: The functioning of pre-Columbian raised-field agriculture and its potential contributions to sustainability today. *Ecol Eng* 45:30–44.
46. Kaplan JO, et al. (2010) Holocene carbon emissions as a result of anthropogenic land cover change. *Holocene* 21(5):775–791.
47. Chave J, et al. (2008) Assessing evidence for a pervasive alteration in tropical tree communities. *PLoS Biol* 6(3):e45.
48. Faegri K, Iversen K (1989) *Textbook of Pollen Analysis* (Blackburn Press, New Jersey).
49. Whitney BS, Rushton EA, Carson JF, Iriarte J, Mayle FE (2012) An improved methodology for the recovery of *Zea mays* and other large crop pollen, with implications for environmental archaeology in the Neotropics. *Holocene* 22(10):1087–1096.

50. Holst I, Moreno JE, Piperno DR (2007) Identification of teosinte, maize, and *Tripsacum* in Mesoamerica by using pollen, starch grains, and phytoliths. *Proc Natl Acad Sci USA* 104(45):17608–17613.

51. Burn M, Mayle FE (2008) Palynological differentiation between genera of the Moraceae family and implications for Amazonian palaeoecology. *Rev Palaeobot Palynol* 149(3-4):187–201.

Supporting information

SI Text

SI Figures. Radiocarbon calibration curves. To construct the age models for both sets of lake cores, single age estimates for each date were derived by calculating the weighted mean of the probability distribution of the calibrated age ranges (1), and an age-depth curve drawn by linear interpolation between those calibrated ages (Figs. S1 and S2). This simple linear interpolation is the most appropriate method, given the small number of dates (2).

Pollen concentration values. Pollen concentration values (Figs. S3 and S4) of key taxa in each lake mirror changes in the percentage abundance diagrams (Figs. 2 and 4), confirming that pollen percentage changes reflect real changes in pollen abundance of a given taxon, rather than a statistical artifact associated with percentage calculations.

Site Descriptions. The seasonal southern Amazonian rainforest. The forests of the southern sub-region of Amazonia, an area of ~1,000,000 km², experience marked seasonality of precipitation in comparison with the western and central Amazon basin (see Fig. 1A in main text). This is the potential area of forest ecotonal movement over the mid-to-late Holocene and, as estimated from the distribution of earthworks discovered so far, the potential area of geometric earthworks that may lie undiscovered beneath the modern rainforest.

The Iténez region. The Iténez province is situated in the northeast of Beni department, Bolivia, extending to the international border with Brazil. Our study sites occur on either side of the confluence between the San Martín and Blanco Rivers (Fig. 1B). This water course marks the geologically defined transition between the higher-elevation terra firme land of the Pre-Cambrian Shield (PCS) to the north and the low-lying, flat sedimentary Beni Basin to the south. The large lobe of the PCS, on which Laguna Granja (LG) is found, covers an estimated 5,500 km² in area. The dominant vegetation type of the PCS lobe is mostly undisturbed, dense, humid, evergreen rainforest, which is floristically linked to the Madeira-Tapajós ecoregion (3) and part of the Iténez Protected Area. The Beni Basin, a vast (135,000 km²) seasonally inundated forest–savanna mosaic, is located to the south and west of the PCS. This low-elevation sedimentary basin contains thick impermeable clay soils (4) overlain with natural savannas that flood seasonally, mostly during the months of November to March, because of the passage of the South American (austral) summer monsoon (SASM). This seasonal inundation restricts forest growth to local non-flooded areas of higher elevation, such as forest islands atop scattered outcrops of the PCS, which occur naturally in the region, but also artificial causeways that were created by pre-Columbian earth-moving cultures (5).

Laguna Granja. LG (13°15'44" S, 63°42'37" W) is an oxbow lake located ~1 km north of the boundary of the modern village of Bella Vista and 300 m from the present course of the San Martín River at its closest margin; it lies on the north, PCS side of the San Martín River. The surface area of the lake is ~0.2 km², with a maximum water depth of 2 m. During the annual wet season the lake margins become flooded up to a height of 2 m, and in some years the lake becomes hydrologically linked to the river. Particle size analysis conducted on the lake sediment core shows no variation in grain size of the sediments, which were composed of clays and very fine sands throughout. This lack of lithological change down core suggests that LG has not been disrupted by river channel migration over the last 6,000 y. Any lateral migration of the river over this time period must have been minimal, as the river course is geographically constrained by the terra firme PCS to the north. The LG site was

selected for its close proximity to archaeological remains, in particular, a ring-ditch site named “Granja del Padre” that lies 100 m from the eastern shore of the lake (Figs. 1C and 3 in main text).

The vegetation immediately around LG is riverine forest, and this forest shows evidence of recent burning and clearance for shifting cultivation. On the east side of the lake, forest has been cleared to create a 0.3-km² area of grassland for cattle ranching. The most abundant terrestrial tree species in the riverine forest are *Vochysia mapirensis* (Vochysiaceae) and *Buchenavia oxycarpa* (Combretaceae). The littoral margins of the lake, especially on its north side, are dominated by floating mats of aquatic vegetation, including the water fern *Marsilea polycarpa* (Marsileaceae) and the water hyacinth *Eichhornia azurea* (Pontederiaceae). The wider area of the PCS surrounding the lake is covered with closed-canopy terra firme evergreen rainforest, which is degraded by modern anthropogenic disturbance to a distance of 5 km from the lake.

L. Orícore. Laguna Orícore (LO) (13°20'44.02”S, 63°31'31.86” W) is one of the large (11.2 km²), shallow, flat-bottomed lakes common in the Beni Basin. Much of the lake margin is fringed by a 10-m-wide strip of seasonally inundated gallery forest. A 1.5-km-wide outcrop of the PCS, currently supporting terra firme forest, and containing some drought-tolerant taxa, is situated at the northeast margin of the lake. Seasonally flooded savannah dominates the wider landscape in which LO is situated, and the margin of the PCS lobe, presently covered by terra firme evergreen humid rainforest, is situated 3 km north of the lake.

Pollen and Charcoal Catchment/Source.

Pollen catchment area. The pollen catchment area of a lake, and therefore the spatial area of terrestrial vegetation represented in the fossil pollen record, is largely proportional to the lake surface area (6). Whereas paleoecological records from very large lakes, several kilometers in diameter, represent vegetation on a regional scale, records from small lakes (e.g., oxbows) represent smaller, local-scale palaeoenvironmental histories. In Iténez we aimed to determine the relative spatial scales of human impact in the ring-ditch region, and therefore selected two lakes of different size for coring, to provide regional- and local-scale records of vegetation/burning. The smaller lake, LG, provides a local-scale palaeoenvironmental record from within the earthwork site, and is nested within the regional-scale pollen catchment area of LO (*see diagram in Fig. S5*).

Pollen and charcoal source. LO receives flood waters (and hence pollen) in the rainy season from both the adjacent seasonally-flooded Beni savannas and San Martín river. However, any pollen inputs to the lake from these flood waters can only constitute a minor proportion of the lake’s total pollen influx, because the surface-sediment pollen assemblage from LO is diagnostic of closed-canopy humid evergreen rainforest, which only exists, at a regional scale, on the PCS north of the San Martín River. This interpretation is based upon the dominance of arboreal rainforest taxa in surface-sediment pollen assemblages, in particular genera of the Moraceae family (*Pseudolmedia*, *Brosimum*, *Helicostylis*, *Maclura*), the pollen of which is wind-dispersed and comprises 60% of the terrestrial pollen sum. The latter closely matches the modern pollen-rain signature of humid evergreen rainforest in the region (collected by artificial traps in 1-ha study plots) (7, 8), and is distinctly different from the modern pollen-rain signatures of both seasonally dry tropical forest and savanna ecosystems (9, 10). We therefore conclude that the fossil pollen record of LO predominantly reflects the vegetation history of the PCS north of the San Martín River. Furthermore, if the main pollen source of LG and LO did come from the San Martín River and its upstream drainage, or the seasonally flooded Beni basin wetlands, one would expect to find very similar fossil pollen records in both lakes, reflecting a

common riverine/wetland source. Analysis of the deeper lake sediments reveals, however, that each site has a distinct fossil pollen record, further demonstrating that the main pollen source is derived from aerial inputs from the PCS. The macroscopic charcoal records from the two lakes are also very different, indicating that charcoal inputs also came from spatially distinct local sources around the lakes, rather than from a common homogenized source of charcoal transported from the south by the river.

Granja charcoal. The influx of macroscopic charcoal to lake basins is complex (11) and variations in the fossil record can result from changes in sedimentation rates. At LG peak total pollen concentration values precede the charcoal peak at 700 B.P. This charcoal peak is constrained by two radiocarbon dates, and our age model shows a linear sedimentation rate throughout zones LG-1 and 2 (see Radiocarbon calibration curves, above). The latter, together with the lack of any lithological changes in the core, indicates that the fluctuations in the charcoal curve represent actual changes in the amount of charcoal entering the lake, rather than a decrease in lake sedimentation rates.

Zea mays pollen representation. *Z. mays* pollen was found in the sediments of LG but not LO. There are two possible explanations for the absence of maize pollen from LO. It may be the case that maize was not grown around the lake margins of LO and therefore does not appear in the pollen record. Alternatively, the lake may be so large and shallow (with little sediment focusing toward the center), that even if maize was grown at the lake shore, its pollen is too poorly dispersed to have reached the core site at the center of the lake.

Coring and Pollen Preservation. A 240-cm core was extracted from LG, including a 58-cm surface core. Sediments consist of uniform light-brown clay throughout. Pollen is well preserved throughout the core, except in horizons between 170 and 150 cm. Pollen/charcoal analyses and radiocarbon dating of sediments were therefore focused above 150 cm, where we could be confident of continuous sedimentation. Overlapping core sections were correlated by wiggle-matching curves from high-resolution (0.5 cm) charcoal analysis.

The LO sediment core measures 120 cm, including a 54-cm surface core. Sediments consist of uniform, stiff, light-gray clay throughout. Pollen analysis was performed on sediments between 0 cm and 40 cm, where concentrations were sufficient for analysis.

Geometric Earthworks. These archaeological features show variations between the three regions of Amazonia where they have been discovered: northeast Bolivia, Acre, and Upper Xingu, Brazil. In Pando department and the Iténez province of northeast Bolivia and the Upper Xingu region in Brazil, the earthworks tend to be simple, circular, ditched enclosures and are typically referred to as “ring ditches” (5, 12, 13). North of the Iténez region, in eastern Acre state, northwest Brazil, the earthworks often have more complex geometric shapes and are referred to as “geoglyphs” (14). For convenience, we refer to all of those features which occur along the seasonal southern Amazonian rainforests (SSAR) (15) collectively as “geometric earthworks.”

In the Iténez province of northeast Bolivia, the ring ditches are part of a wider landscape of earthwork features. These include causeway features which cross the seasonally flooded Beni savannahs, linking up small terra firme outcrops of the PCS or “forest islands.” In the south of the Iténez province, around the town of Baures, Erickson (16) has identified networks of zigzagged earthwork features and small ponds which functioned as fish weirs.

Mid-Late Holocene Climate Change. There is widespread evidence from a suite of different paleoclimatic proxy data that southwest Amazonia and the adjacent tropical Andes were significantly drier than present during the middle Holocene, approximately 8000–4000 cal yr B.P., with peak

drying centered around 6000 cal yr B.P. Most of these data come from the high Bolivian/Peruvian Andes; for example, peak dust concentrations and snow accumulation minima in the Sajama mountain ice cores (17), oxygen isotope ratios in lacustrine calcite (18), and most convincingly, diatom, geochemical, and seismic evidence for lake-level lowstands, particularly in Lake Titicaca (19), where lake level dropped to 100 m below present between 6000–5000 cal yr B.P. The broad trend of increasing precipitation since the mid-Holocene is consistent with the 20,000-y precession orbital cycle (20) as the dominant driver of tropical climate, causing progressively greater austral summer insolation, and hence a stronger SASM, through the Holocene. Although these paleoclimatic records come from sites in the tropical high Andes, they are representative of our lowland study area because they receive most of their precipitation from the Amazon lowlands via the SASM. One can therefore view Lake Titicaca as a key “rain gauge” for southwest Amazonia, at least with respect to the direction of precipitation change through the Holocene (19).

More direct evidence that lowland eastern Bolivia experienced drier mid-Holocene conditions compared with present comes from a range of paleoenvironmental proxies. Geomorphological data from the Andean piedmont and foreland basin reveal increased fluvial-aeolian sedimentation and aggradation, parabolic paleodune systems, large-scale river-channel shifts, as well as paleosol-sediment changes, all of which have been interpreted as evidence of drier mid-Holocene climatic conditions with more episodic rainfall and increased aeolian activity caused by reduced vegetation cover (21–24). Paleo-limnological data from two lakes in lowland Bolivia also reveal reduced mid-Holocene precipitation: expansion of shallow-water species of *Pediastrum* algae (25) and semiemergent aquatic plants (*Isoetes*) (26, 27), both signifying lake-level reductions.

SI Methods

Sediment Acquisition. Fieldwork was carried out in June–July 2011. Samples were taken from a stable floating platform in the central, deepest part of both lakes using a drop-hammer Colinvaux-Vohnout modified Livingston piston corer (28, 29). A 5-cm diameter Perspex tube was used to capture the surface core, including the uppermost unconsolidated sediments. Softer sediments from the surface core were divided in the field into 0.5-cm increments and stored in watertight plastic tubes. Firmer sediments were extruded as intact cores in the field and shipped back to the United Kingdom in robust, watertight packaging. Livingstone core sections were transported in their aluminium core tubes and extruded in the laboratory in the United Kingdom. In the laboratory the sediment cores were split lengthways into equal core halves, one of which was used for destructive sampling while the other was retained as an archive core. All samples were kept in cold storage at 4 °C.

Lab Protocol: Pollen Analysis. The LG core was subsampled for pollen analysis at 5-cm intervals between 0- and 110-cm depth (0 to ~3300 cal yr B.P.) and at 10-cm intervals between 110- and 150-cm depth (3000 to ~6100 cal yr B.P.). The LO core was subsampled at 1-cm intervals between 0- and 22-cm depth (0 to ~2550 cal yr B.P.) and at 2- to 3-cm intervals between 22- and 40- cm depth (~2550 to ~6700 cal yr B.P.). A 1-cm³ subsample of sediment was prepped from each horizon using a modified sieving protocol designed for optimal recovery of large cultigen pollen (30). All other stages follow the standard pollen preparation protocol (31). Samples were spiked with a known concentration of *Lycopodium* marker spores for calculation of pollen concentration. Pollen concentration values were calculated from pollen samples from sediment cores in both lakes to confirm that observed changes in pollen percentage abundance in the paleo record were not the result of changes within a closed sum. The pollen in the fine fractions (material < 53 µm) was counted to the

standard 300 terrestrial grains. The coarse fractions were scanned for pollen up to a standardized equivalent count of 2,000 Lycopodium grains, representing ~0.4 cm³ of sediment scanned. Fossil pollen was identified with reference to the modern pollen collection of over 1,000 South American tropical rainforest, dry forest, and savanna taxa housed at the University of Edinburgh and University of Reading. Maize pollen grains were distinguished from those of other wild grasses according to the morphological criteria described in Holst et al. (32). Where possible, members of the Moraceae family were identified to genus using pollen reference material and morphological descriptions from Burn and Mayle (33). Where genus level identification was not possible, grains were assigned to the Moraceae/Urticaceae undifferentiated category.

In a botanical survey of the modern vegetation surrounding LG conducted by J.D.S., Cyperaceae—which can be both a terrestrial and an aquatic herb—was identified exclusively as an aquatic/semiaquatic type on the lake margins. Cyperaceae pollen in the LG assemblages was therefore classified as an “aquatic” type and excluded from the terrestrial pollen sum of 300 grains. (Note: The inclusion/exclusion of Cyperaceae pollen from the terrestrial pollen sum was found to have a negligible impact upon the pattern of the arboreal pollen rise seen in the LG record at 500 B.P.). Cyperaceae, however, is known to be an important taxon in the seasonally flooded Beni savanna (10), which surrounds LO; therefore, its pollen was included in the terrestrial count of 300 grains from LO.

Charcoal Analysis. Samples for charcoal analysis were initially taken at 10-cm intervals, and after preliminary analysis, sampling resolution for charcoal analysis was increased where significant vegetation changes or burning were recognized. The final sampling strategy for LG was at every 0.5-cm interval from 0- to 110-cm depth, and in the remainder of the core where charcoal abundance was consistently low, sampling resolution was lowered to 5-cm intervals. LO was subsampled at 0.5-cm intervals from 0- to 40-cm depth.

Charcoal analysis was performed on subsamples of 1 cm³ that were first treated with hot 10% (wt/vol) sodium pyrophosphate for 10 min to disaggregate the clayey sediments. The samples were then sieved using 250- μ m and 125- μ m nested sieves, and charcoal particles from each recovered fraction were counted in water under 40 \times magnification.

SI References

1. Telford RJ, Heegaard E, Birks HJB (2004) The intercept is a poor estimate of a calibrated radiocarbon age. *Holocene* 14(2):296–298.
2. Telford RJ, Heegaard E, Birks HJB (2004) All age–depth models are wrong: But how badly? *Quat Sci Rev* 23(1-2):1–5.
3. Navarro G, Maldonado M (2005) *Geografía Ecología de Bolivia: Vegetación y Ambientes Acuáticos* [Ecological Geography of Bolivia: Vegetation and Aquatic Environments] (Centro de ecología difusión de simion I, Patino, Santa Cruz, Bolivia). Spanish.
4. Clapperton CM (1993) *Quaternary Geology and Geomorphology of South America* (Elsevier Science, Amsterdam).
5. Erickson C (2010) The transformation of environment into landscape: The Historical Ecology of monumental earthwork construction in the Bolivian Amazon. *Diversity* 2(4):618–652.
6. Sugita S (1994) Pollen representation of vegetation in Quaternary sediments: Theory and method in patchy vegetation. *J Ecol* 82(4):881–897.
7. Burn M, Mayle FE, Killeen T (2010) Pollen-based differentiation of Amazonian rainforest communities and implications for lowland palaeoecology in tropical South America. *Palaeogeogr Palaeoclimatol Palaeoecol* 295(1-2):1–18.
8. Gosling W, Mayle FE, Tate N, Killeen T (2005) Modern pollen-rain characteristics of tall terra firme moist evergreen forest, southern Amazonia. *Quat Res* 64(3):284–297.
9. Gosling W, Mayle FE, Tate N, Killeen T (2009) Differentiation between Neotropical rainforest, dry forest, and savannah ecosystems by their modern pollen spectra and implications for the fossil pollen record. *Rev Palaeobot Palynol* 153(1-2):70–85.
10. Jones H, Mayle FE, Pennington RT, Killeen T (2011) Characterisation of Bolivian savanna ecosystems by their modern pollen rain and implications for fossil pollen records. *Rev Palaeobot Palynol* 164(3-4):223–237.
11. Whitlock C, Larsen C (2001) in *Tracking Environmental Change Using Lake Sediments*, eds Smol JP, Birks HJB, Last WM (Kluwer Academic, Dordrecht), Vol 3, pp 75–96.
12. Saunaluoma S (2010) Pre-Columbian earthworks in the Riberalta region of the Bolivian Amazon. *Amazonica* 2(1):104–138.
13. Heckenberger MJ, et al. (2008) Pre-Columbian urbanism, anthropogenic landscapes, and the future of the Amazon. *Science* 321(5893):1214–1217.
14. Parssinen M, Schaan D, Ranzi A (2009) Pre-Columbian geometric earthworks in the upper Purús: A complex society in western Amazonia. *Antiquity* 83(322):1084–1095.
15. Mann CC (2008) Archaeology. Ancient earthmovers of the Amazon. *Science* 321(5893):1148–1152.
16. Erickson CL (2000) An artificial landscape-scale fishery in the Bolivian Amazon. *Nature* 408(6809):190–193.
17. Thompson LG, et al. (1998) A 25,000-year tropical climate history from Bolivian ice cores. *Science* 282(5395):1858–1864.

18. Seltzer GO, Rodbell D, Burns SJ (2000) Isotopic evidence for late Quaternary climatic change in tropical South America. *Geology* 28(1):35–38.
19. Baker PA, et al. (2001) The history of South American tropical precipitation for the past 25,000 years. *Science* 291(5504):640–643.
20. Berger A, Loutre MF (1991) Insolation values for the climate of the last 10 million years. *Quat Sci Rev* 10(4):297–317.
21. May J-H (2006) Geomorphological indicators of large-scale climatic changes in the eastern Bolivian lowlands. *Geogr Helv* 61(2):120–134.
22. May J-H, Argollo J, Veit H (2008) Holocene landscape evolution along the Andean piedmont, Bolivian Chaco. *Palaeogeogr Palaeoclimatol Palaeoecol* 260(3-4):505–520.
23. May J-H, Veit H (2009) Late Quaternary paleosols and their palaeoenvironmental significance along the Andean piedmont, Eastern Bolivia. *Catena* 78(2):100–116.
24. Servant M (1981) Phases climatiques arides holocenes dans le sud-ouest de l'Amazonie [Arid climatic phases of the Holocene in south-west Amazonia (Bolivie)]. *CR Acad Sc Paris Ser II* 292:1295–1297.
25. Whitney BS, Mayle FE (2012) *Pediastrum* species as potential indicators of lake-level change in tropical South America. *J Paleolimnol* 47(4):601–615.
26. Mayle FE, Burbridge R, Killeen TJ (2000) Millennial-scale dynamics of southern Amazonian rain forests. *Science* 290(5500):2291–2294.
27. Burbridge R, Mayle FE, Killeen T (2004) Fifty-thousand-year vegetation and climate history of Noel Kempff Mercado National Park, Bolivian Amazon. *Quat Res* 61(2):215–230.
28. Wright HEJ (1967) A square-rod piston sampler for lake sediments. *J Sediment Petrol* 37(3):957–976.
29. Colinvaux P, de Oliveira PE, Partino JEM (1999) *Amazon Pollen Manual and Atlas* (Harwood Academic, Amsterdam).
30. Whitney BS, Rushton EA, Carson JF, Iriarte J, Mayle FE (2012) An improved methodology for the recovery of *Zea* mays and other large crop pollen, with implications for environmental archaeology in the Neotropics. *Holocene* 22(10):1087–1096.
31. Faegri K, Iversen K (1989) *Textbook of Pollen Analysis* (Blackburn Press, New Jersey).
32. Holst I, Moreno JE, Piperno DR (2007) Identification of teosinte, maize, and *Tripsacum* in Mesoamerica by using pollen, starch grains, and phytoliths. *Proc Natl Acad Sci USA* 104(45):17608–17613.
33. Burn M, Mayle FE (2008) Palynological differentiation between genera of the Moraceae family and implications for Amazonian palaeoecology. *Rev Palaeobot Palynol* 149(3-4):187–201.

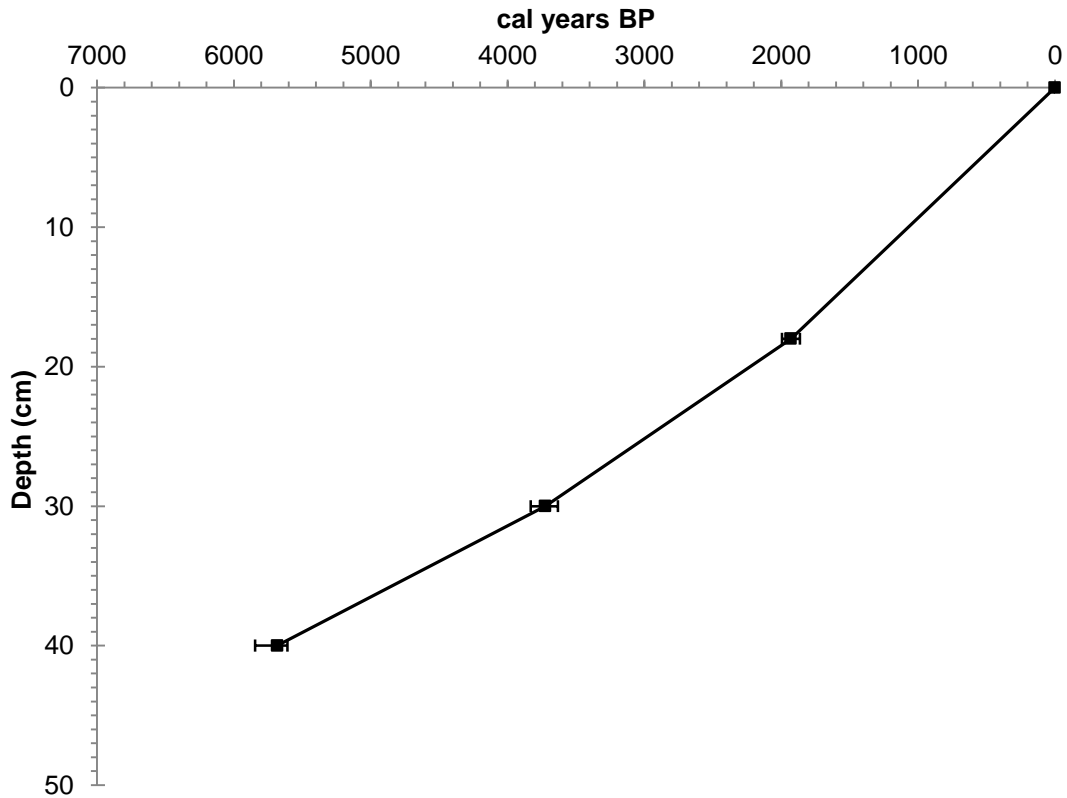


Fig. S1. Age-depth model for LO core, based on linear interpolation between three calibrated AMS radiocarbon dates (Table S1). Error bars represent 2σ (95%) calibrated age ranges. Surface sediment is assumed to be modern or 0 y B.P.

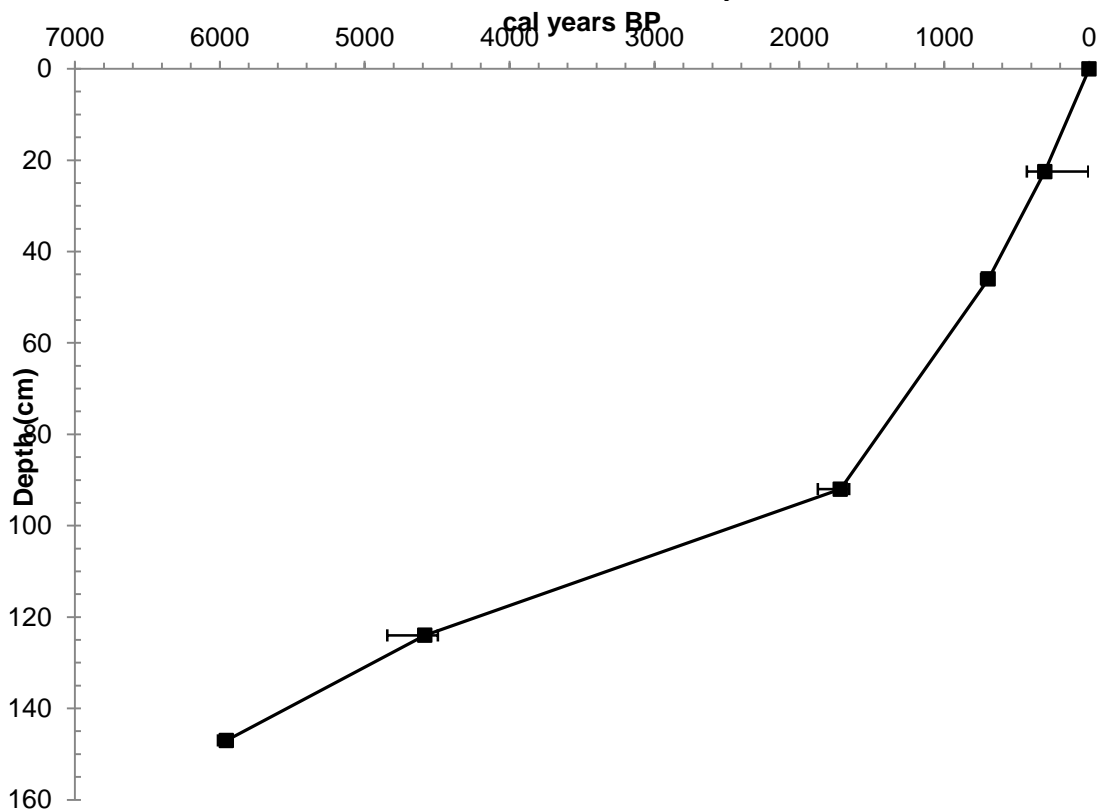


Fig. S2. Age-depth model for LG core, based on linear interpolation between five calibrated AMS radiocarbon dates (Table S1). Error bars represent 2σ (95%) calibrated age ranges. Surface sediment is assumed to be modern or 0 y B.P.

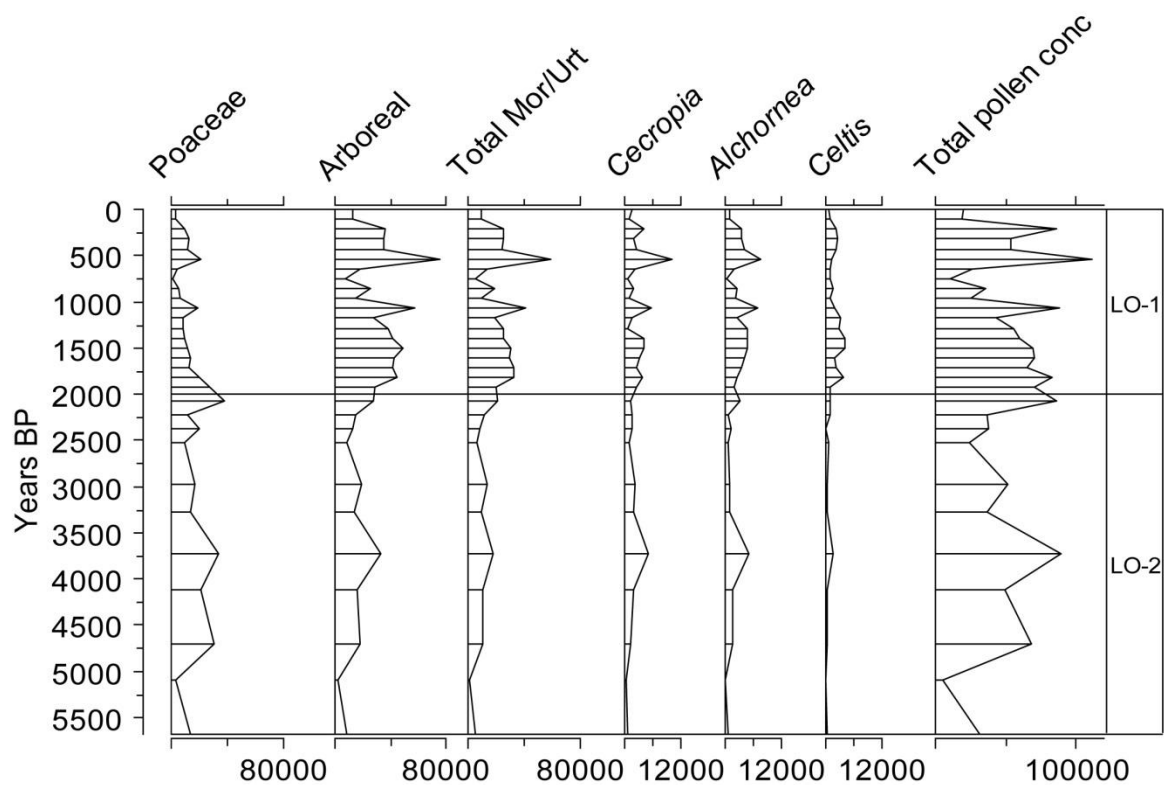


Fig. S3. Pollen concentration values from LO. Key pollen taxa and total arboreal pollen are shown alongside total pollen concentrations. Presented as number of grains per cubic centimetre of sediment.

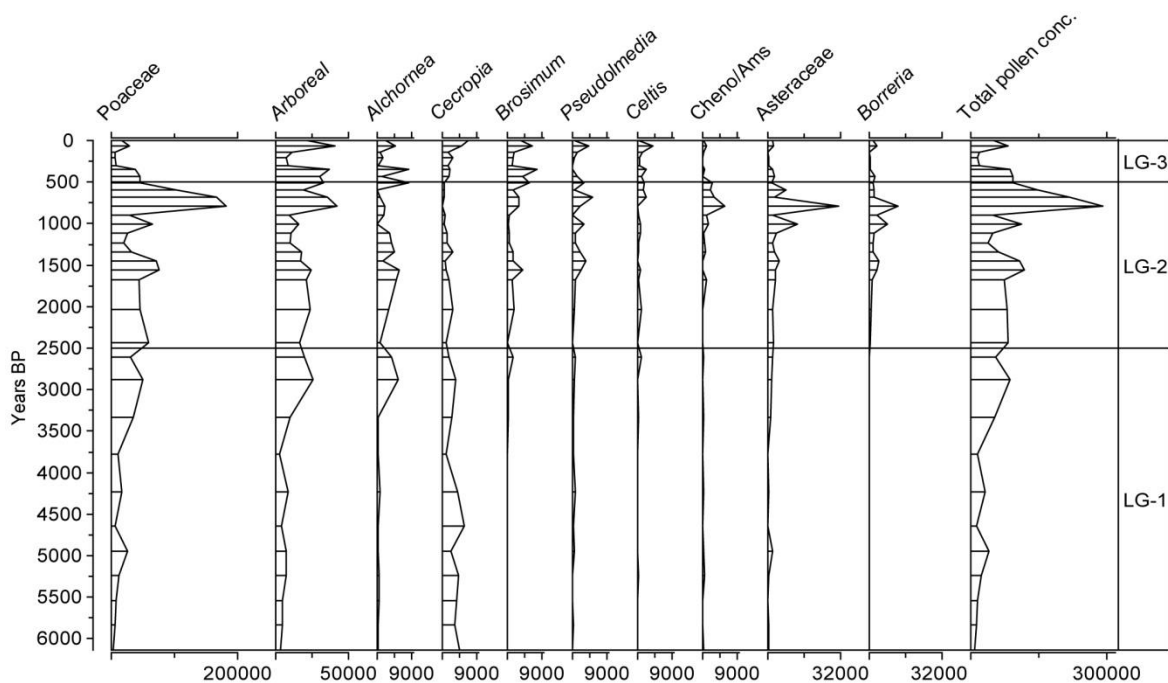


Fig. S4. Pollen concentration values from LG. Key pollen taxa and total arboreal pollen are shown against total pollen concentrations. Presented as number of grains per cubic centimeter of sediment.

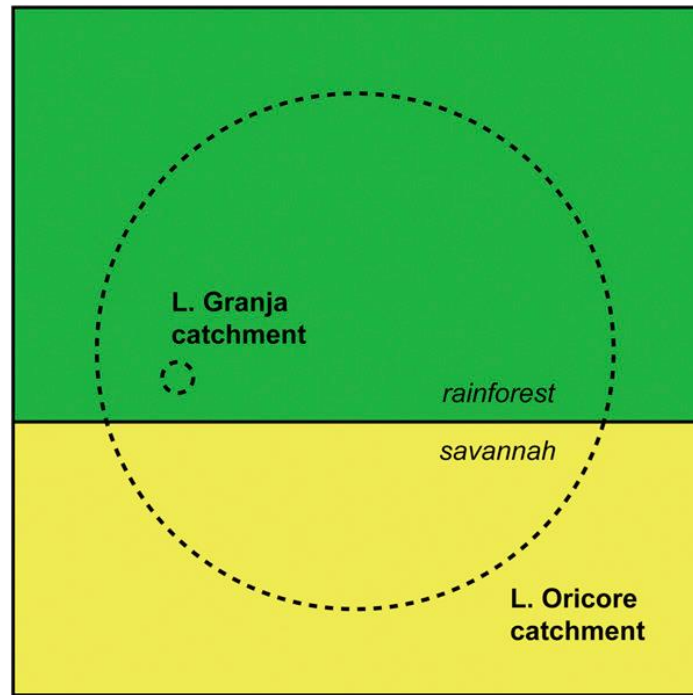


Fig. S5. Schematic representation of LG pollen catchment area, nested within the LO pollen catchment.

Table S1. AMS ^{14}C dates

Site and sample identifier	Publication code	Depth below sediment-water interface (cm)	Conventional C^{14} age (yr BP $\pm 1\sigma$)	Calibrated age range (cal yr BP) $\pm 2\sigma$	Area under probability curve	Weighted mean calibration (cal yr BP)	$\delta^{13}\text{C}_{\text{VPDB}}(\text{‰})$
Granja Gr 21.5	Beta - 339227	21.5-22.5	240 ± 30	430-357	0.299	306	-26.4
				332-280	0.547		
				170-150	0.131		
				11-0	0.023		
Granja Gr45	Beta - 339228	45-45	750 ± 30	730-660	1	696	-23.1
Granja Gr 91	SUERC-43148	91-92	1782 ± 38	1820-1610	1	1716	-22.2
Granja Gr123	Beta-347192	123-124	4070 ± 30	4800-4770	0.128	4585	-23.3
				4700-4670	0.021		
				4650-4500	0.691		
				4490-4440	0.160		
Granja GR 146	Beta - 339229	146-147	5200 ± 30	6000-5910	1	5954	-24.2
Oricore Or 17-18	Beta-339231	17-18	1970 ± 30	1995-1865	1	1930	-19.9
Oricore Or 29-10	Beta 347194	29-30	3440 ± 30	3830-3790	0.176	3725	-26.1
				3780-3630	0.824		
Oricore Or 39-40	Beta 339232	39-40	4970 ± 30	5840-5780 5750-5610	0.020 0.980	5683	-19.8

Five radiocarbon dates were obtained to construct a chronology for LG and three dates for LO. All dates were obtained from noncalcareous bulk sediments and the results are presented in the table. The dates were calibrated using the IntCal09 calibration curve in OxCal v4.1 (1). The 2σ (95%) calibrated age ranges of each date are presented. Single age estimates for each date were calculated from the weighted means of the probability distribution of the calibrated age ranges (2).

1. Bronk Ramsey C (2009) Bayesian analysis of radiocarbon dates. Radiocarbon 51(1):337–360.

2. Telford RJ, Heegaard E, Birks HJB (2004) The intercept is a poor estimate of a calibrated radiocarbon age. Holocene 14(2):296–298.